PERIODICITIES OF SOLAR IRRADIANCE AND SOLAR ACTIVITY INDICES, II

S. D. BOUWER

NOAA Space Environment Laboratory, System Technology Associates, Inc., Boulder CO 80303, U.S.A.

(Received 21 May, 1991; in revised form 28 April, 1992)

Abstract. Using a dynamic power spectral analysis technique, the time-varying nature of solar periodicities is investigated for background X-ray flux, 10.7 cm flux, several indices to UV chromospheric flux, total solar irradiance, projected sunspot areas, and a sunspot blocking function. Many prior studies by a host of authors have differed over a wide range on solar periodicities. This investigation was designed to help resolve the differences by examining how periodicities change over time, and how the power spectra of solar data depend on the layer of the solar atmosphere. Using contour diagrams that show the percent of total power over time for periods ranging from 8 to 400 days, the transitory nature of solar periodicities is demonstrated, including periods at 12–14, 26–28, 51–52, and approximately 154 days. Results indicate that indices related to strong magnetic fields show the greatest variation in the number of periodicities, seldom persist for more than three solar rotations, and are highly variable in their frequency and amplitude. Periodicities found in the chromospheric indices are fewer, persist for up to 8–12 solar rotations, and are more stable in their frequency and amplitude. An additional result, found in all indices to varying degrees and related to the combined effects of solar rotation and active region evolution, is the fashion in which periodicities vary from about 20 to 36 days. I conclude that the solar data examined here are both quasi-periodic and quasi-stationary, with chromospheric indices showing the longest intervals of stationarity, and data representing strong magnetic fields showing the least stationarity. These results may have important implications to the results of linear statistical analysis techniques that assume stationarity, and in the interpretation of time series studies of solar variability.

1. Introduction

Since the development of various time series analysis techniques, there have been hundreds of studies revealing the various periodicities in various solar data. The existence of the 11-year solar cycle and the 27-day solar rotational period is well known in different solar indices. Additional periodicities around 300, 150, 51, and 13.5 days have been reported by numerous authors (e.g., Ichimoto *et al.*, 1985; Bai, 1987a,b; Lean and Brueckner, 1989; Pap, Tobiska, and Bouwer, 1990; Donnelly and Puga, 1990). However, the studies of solar periodicities show different results depending on the particular data set used and the time interval analyzed. These discrepancies are partly related to the different physical origins of the various solar indices and to the limitations in the interpretation of power spectral analysis of data containing quasi-periodic and quasi-stationary solar phenomena.

Pap, Tobiska, and Bouwer (1990; hereafter referred to as 'Paper I' of this study) explored the periodicities resulting from a standard fast-Fourier analysis of certain solar indices, such as solar and UV irradiances, 10.7 cm radio flux, Ca-K plage index, projected areas of young developing and old decaying sunspots, and the sunspot blocking function. It was shown that an 8–11-month period exists in the total and UV irradiances, 10.7 cm radio flux, plage index, and sunspot blocking function. Periods at

Solar Physics **142:** 365–389, 1992.

154 and 51 days were found in those solar data that are related to strong magnetic fields. Paper I also demonstrated that the 27-day rotational period is more pronounced during the declining portion of the solar cycle than during its rising portion. The main purpose here is to examine in greater detail the time dependence of the main periods found in various solar indices corresponding to different layers of the solar atmosphere. Besides the solar data listed above, I also examine the full-disk equivalent width of the He I line at 1083 nm (Harvey, 1984) and solar X-ray flux measured by the GOES satellites in the 1–8 Å spectral band (Wagner, 1988).

In prior studies of solar time series, the term 'quasi-periodicity' often refers to observed solar periodicities that sometimes appear with a dominant frequency, but that also vary in amplitude and frequency throughout the solar cycle (Karlický, 1977; Lean and Repoff, 1987; Harvey, 1984; Heath, Repoff, and Donnelly, 1984). A related term is 'quasi-stationary', defined as a process in which the statistical properties (i.e., the mean, variance, and autocorrelation) of the data depend on a shift in the time origin (Papoulis, 1977). Quasi-periodic and quasi-stationary data representing solar variability tend to change in such a fashion that the results from some linear analysis techniques may be adversely affected. For example, simple linear regressions between two quasi-stationary solar indices may result in a linear expression that fails to accurately represent a relationship, despite a high correlation coefficient.

Typically, a quasi-periodic variation is called quasi-stationary, but here I wish to make a distinction between a periodicity that slowly varies in amplitude and frequency over time and a process in which periodicities dramatically change from one time episode to another, usually without phase coherence between each episode's periodicities. In the discussions that follow, I also distinguish between a periodicity and a non-periodic variation that resembles a waveform. A periodicity is a repeated cyclic phenomenon, while a non-periodic waveform is not cyclical but still can produce a broad peak, centered at a particular frequency in a power spectrum.

Most natural processes are assumed to be weakly stationary if the mean and autocorrelation do not depend on a shift in the time origin (Koopmans, 1974; Bath, 1974). Quasi-stationarity is defined as a weakly stationary process in which the statistical properties are *slowly* varying within the time series (Papoulis, 1977). A second definition of quasi-stationarity, proposed here, concerns processes that are weakly stationary for short episodes of time but that *suddenly* change into a completely different state (i.e., different frequency, phase, and amplitude of periodicities) during the next episode. Additionally, sudden changes in the stationarity of a time series can suggest that an entirely different process dominates a distinct portion of the time series. In solar time series, these episodes tend to correspond to major outbreaks of active regions.

In Bouwer (1983) I suggested that the second type of quasi-stationarity dominates solar variability, based on an analysis of background X-ray flux (X_b). He describes these episodes of activity, lasting 3–6 solar rotations, as 'intermediate-term epochs' with an average duration of 4.5 solar rotations. These intermediate-term episodes correspond to the 'secondary fluctuations' in the Ca-K plage index described by Dodson and Hedeman (1970), who reported no regular pattern in the occurrence of the fluctuations.

As groups of active regions form and decay, they generally persist with strong emissions in most wavelengths up to 3–5 solar rotations and decrease in amplitude. Chromospheric emissions generally persist longer than coronal emissions (Donnelly, 1987). Furthermore, Heath, Repoff, and Donnelly (1984), Harvey (1983), and Donnelly (1987) have shown that the persistence of rotational variations in solar UV flux is generally shorter than nine solar rotations. However, a number of studies have described intermediate-term variations as long as ten solar rotations (Lean and Brueckner, 1989; Harvey, 1984; Donnelly, 1989).

An essential question is whether the intermediate-term epochs are themselves periodic in some fashion. The analysis of a sufficiently long time series may possibly reveal intermediate-term periodicities. Another question is the extent to which periodicities remain constant in frequency and amplitude during an interval of stationarity, especially 27–28-day rotational periods. Finally, there is the question of how periodicities vary among coronal, chromospheric, and photospheric indices during the same time interval. In the discussions that follow, the dynamic power spectra are divided into three time scales: (1) short-term periodicities, with variations between 12 to 38 days; (2) mid-term variations, with a range of 39 to 71 days; and (3) intermediate-term variations, from 72 to 300 days in duration.

2. Data Base

This analysis examines solar irradiance measurements emitted from different layers of the solar atmosphere. The various time series are shown in Figure 1, and are stacked in approximate order of the solar layer: starting from the hot X-ray flux of the lower corona, proceeding down through the chromospheric region as measured by plage and UV flux, then on to the photosphere where the strong magnetic fields form sunspots. Additional data (full-disk 1–8 Å X-ray flux and He I line measurements) are included in this study that were not studied in Paper I.

Since most of the solar indices are described in detail in Paper I, only a brief description is given here. The 10.7 cm radio flux ($F_{10.7}$) and the Ca-K plage index (Ca-K) are published in the NOAA/World Data Center *Solar Geophysical Data Catalogue*. The projected areas of active (S_{act}) and passive (S_{pas}) spots have been calculated by Pap (1986). The active spots are defined as developing, complex sunspot groups, while the passive spots are the old, decaying spots. The total solar irradiance (S) is measured by the ACRIM radiometer on the Solar Maximum Mission satellite (Willson and Hudson, 1988). Another source of sunspot data used in this study is the Photometric Sunspot Index (PSI), which has been calculated by Hudson (1988). PSI relates the observed sunspot areas, and their contrast, to a net effect on the radiative output of the observed solar hemisphere, and it is corrected for limb darkening.

The Mg II center-to-wing ratio data ($R_{Mg\,II}$) have been extended in this study. In Paper I, the data were based on the NIMBUS-7 satellite measurements by Heath and Schlesinger (1986). Here the equivalent NOAA-9 satellite measurements have been normalized to NIMBUS-7 measurements during solar minimum and added to the

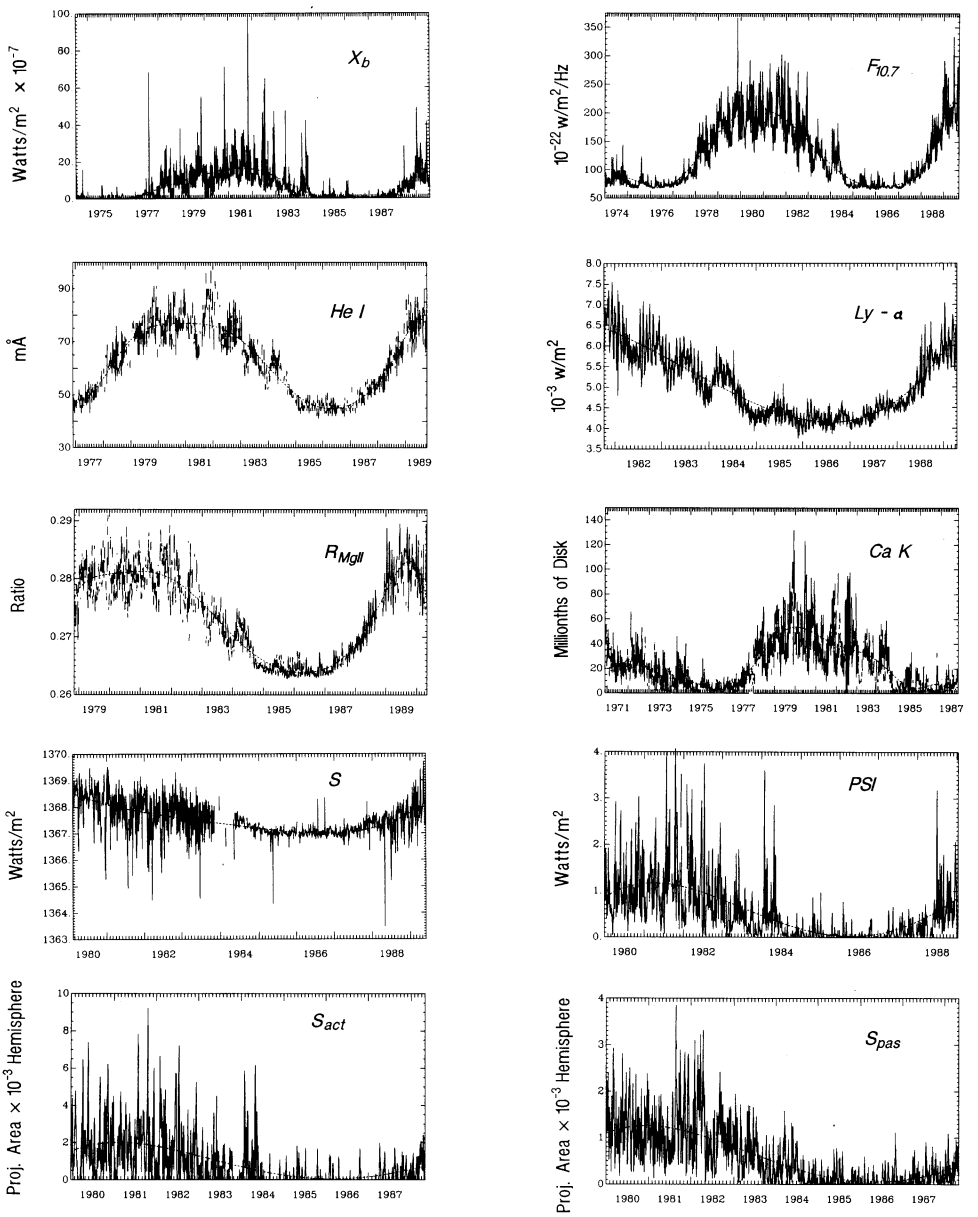

Fig. 1. Solar time series analyzed, with the corresponding nth-order polynomial used to remove the solar-cycle component. All measurements are sampled daily, corrected to a terrestrial perspective at 1 AU. The order of the plots approximately follows the relative solar source regime, in decreasing height. X_b, $F_{10.7}$, He I, and Ca-K were detrended with a 12th-order polynomial, $R_{\mathrm{Mg\,II}}$ with an 8th-order polynomial, and Lα, S, PSI, S_{act}, and S_{pas} with a 4th-order polynomial.

NIMBUS-7 data (Donnelly, 1988, 1992). As an index to daily chromospheric variations since 1979, $R_{\text{Mg II}}$ is an excellent candidate because of its long-term stability and high signal-to-noise properties of the measurement.

One additional measurement is the X-ray flux in the 1–8 Å spectral band, which is emitted in the low solar corona at temperatures above 3×10^6 K and is measured by a series of GOES satellites (Wagner, 1988). The original hourly averaged GOES data are adjusted to reduce the strong effect of solar flares (see details in Bouwer *et al.*, 1982) and are used in this study as the daily background flux (X_b). The second additional measurement is the full-disk equivalent width of the He I line at 1083 nm, which is measured at the National Solar Observatory at Kitt Peak. Harvey (1980, 1984) has found that He I correlates well with the full-disk Ca-K index ($r = 0.94$, and the residuals do not seem to be highly autocorrelated); thus it is used here as a chromospheric index of both plage and active network radiations.

3. Analysis Description

The basic power spectrum employed here is described in detail by Lean and Repoff (1987). One of the advantages of this particular algorithm is that the power spectrum is computed without interpolating missing values present in the time series data. I begin the computations by first removing the solar cycle variation from the time series of length N using an nth-order polynomial, which is shown in Figure 1. One possible problem is that spectral peaks may be introduced by the nth-order polynomial used to remove the long-term solar cycle trends, particularly those with measurements that have a flat solar-minimum background (e.g., X_b, $F_{10.7}$, S_{act}, S_{pas}, PSI). Detrending with a polynomial solar time series that have a flat solar minimum background can generate low-frequency power. This effect has been nearly eliminated by a careful selection of the detrending polynomial. A modified autocorrelation function is then calculated and multiplied by a cosine-bell window (Bloomfield, 1976). The cosine-bell window is unity for 40% of the length of the data window W, then bent down to zero. This tapering effectively reduces spurious sidelobes due to spectral leakage. The modified autocorrelation is calculated up to lag $N/2$ using an algorithm that accounts for missing data. Zeros are then added to the end of the modified autocorrelation, to remove the jagged appearance of the spectral plots and to more accurately estimate the spectral peaks. The power spectral density is calculated by computing the fast-Fourier transform (FFT) of the modified autocorrelation. The sum of absolute power is calculated after a small constant background noise term is subtracted from each term in the spectrum, and the power is reported as the percent of the total power at each frequency. It is the *relative* power of dominant frequencies with respect to non-periodic variations and not the *absolute* power that is important in the discussions that follow. In other words, it can be demonstrated that calculating the percent of total power is conceptually similar to considering only the portion of the absolute power spectrum that is statistically significant.

To study the time-varying behavior of time series, a dynamic power spectrum is

calculated by computing the power spectral density for a time window that is W days long, as described above ($W \ll N$), then successively stepping the window through the data at $W/2$ or $W/4$ steps in time. Using a spatial triangulation algorithm, a contour plot of the power as a function of time and frequency is developed that gives an overall picture of how the power spectrum changes with time. In effect, the contour plots of the dynamic power spectra are like a contour map of a mountainous terrain, with the most power at a particular time and frequency appearing as a 'spectral peak'. This dynamic spectral analysis (also called short-time Fourier transform, or windowed frequency analysis), is one of two techniques used to study time-dependent signals. A second, more recent technique called the 'wavelet transform' produces greater time resolution at high frequencies (Daubechies, 1990).

The contour plots of the various solar indices are shown in Figures 2 to 15. As the window is stepped in time, the data corresponding to the center of the window is marked on the vertical axis. The synodic period in days is shown on the bottom axis. Figures 2 to 11 show the short- and mid-term dynamic power spectra, using a window $W = 256$ days to describe solar variations from 11 days to about 200 days, and stepping the time window by 64 days. The time interval analyzed is a subset of the original time series, selected so that the same 1981–1987 time period is covered by all ten indices. Figures 12 to 15 give the power spectra of selected time series using a window $W = 512$ days to describe intermediate-term solar variations from 66 days to about 300 days, stepping the window 128 days during the 1975–1986 time interval.

The contour lines shown in Figures 2 to 14 begin just above the estimated level that can be attributed to randomly distributed noise. For short-term and mid-range variations (i.e., 12–71 days), the estimated signal noise was typically near 0.5% of total power. While analyzing the noise properties of the data analysis using random and quasi-stationary test data, I found that signal noise could most easily be estimated by visually inspecting the contour plots, interpreting random and broadly dispersed spectral peaks at low power levels as signal noise. The advantage of presenting the dynamic power spectra as a percent of total power is that this method displays only those periodicities (or singular events of a particular waveform) that dominate the variance of a time series of length W. Furthermore, since the variance of the solar time series typically decreases during solar minimum, presenting the relative power instead of the absolute power visually compensates for this change in the variance and presents a consistent power spectrum over time. Finally, note that the results are accurate in time only to within a fraction of the data window (i.e., approximately $W/4$). The accuracy in the frequency of a periodicity corresponds to less than a one-day error at about 27 days, increasing to about a ten-day error at 150 days.

The statistical reliability of the dynamic power spectra is difficult to determine because of the quasi-stationary nature of the data. Since the calculations of power spectra and tests of significance both assume stationarity in some sense, quasi-stationarity will affect both results. However, one can reasonably assume that the spectral peaks are quite real because: (1) only the power that exceeds spectral noise is presented in the contour figures (the noise was estimated from test cases of known signal and noise properties);

(2) several observed periodicities were tested with more traditional methods (for example, I found that the 51-day period in S_{act} for several early episodes was significant at the 68% confidence level, using running power spectra from Welsh, 1967); and (3) a spectral peak that persists in more than one independent data set increases in statistical significance (see 'Combining Significance Tests', Kotz and Johnson, 1983). Consequently, the periodicities reported here that occur at several times and in several indices increase rapidly in statistical significance with each sample set, and there can be little doubt they represent solar variations and are not an artifact of measurement noise or analysis limitations.

4. Results of Time Series Analysis

At first inspection, the results of the dynamic power spectra (Figures 2–15) are complicated and difficult to interpret. Closer examination reveals that indices related to chromospheric emissions (i.e., $F_{10.7}$, He I, Lα, $R_{Mg\,II}$, Ca-K, Figures 3–7) show the most consistent and stationary spectral peaks, particularly at the 27–28-day solar rotational period. The coronal emissions of X_b (Figure 2) produce dynamic power spectra dominated by intermediate-term spectral peaks and short-lived periodicities between

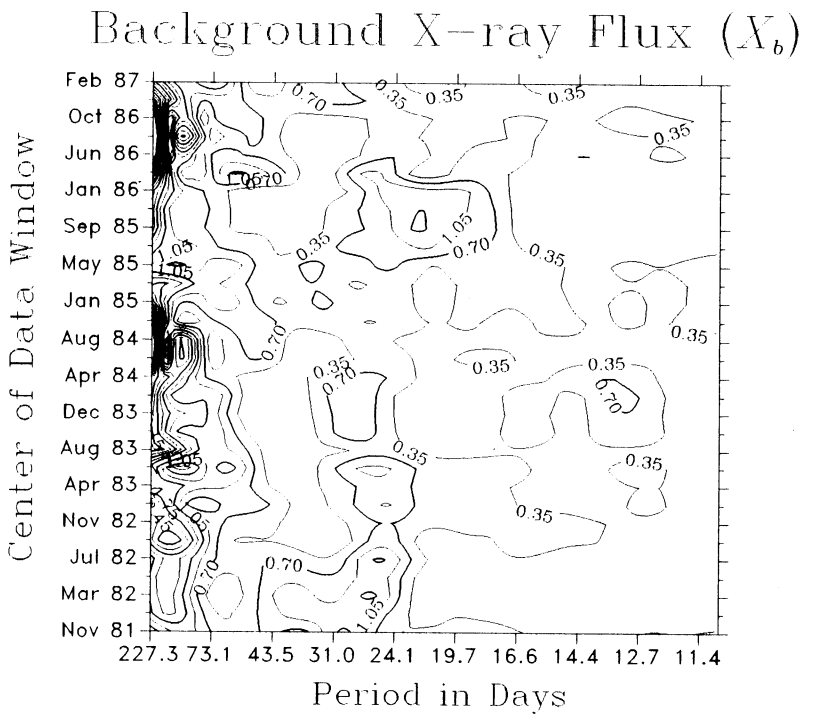

Fig. 2. Dynamic power spectra of the background X-ray index to full-disk X-ray flux in the 1–8 Å range, emphasizing short-term periodicities related to solar rotation. Contour levels are in units of percent of total power, for a data transform window 256 days long, stepping every 64 days.

18–40 days. The interrelated photospheric indices (S, PSI, S_{act}, S_{pas}, Figures 8–11) show distinct, isolated spectral peaks at unexpected periods. Recall that our use here of the expression 'rotational periodicities' means the apparent rotational periodicities resulting from 27–28-day solar rotation that is subsequently modulated in frequency and amplitude by the evolution of major solar features. For the interested reader, it is very helpful to align copies of the figures on a large poster for comparison. The remainder of this section highlights the observational results of individual indices, and Section 5 discusses common spectral peaks.

4.1. Background 1–8 Å X-ray

Results of the full-disk X-ray background flux, X_b, are shown in Figures 2 and 12. Recall that during solar minimum (i.e., 1975–1976 and 1985–1986) X_b is at very low flux levels. At such low flux levels the X-ray detectors on the GOES satellites are subject to relatively large errors (Bouwer *et al.*, 1982). Thus, the signal-to-noise level of X_b is favorable only during times other than solar minimum. Note how intermediate-term variations (i.e., approximately 81–300 days) in X_b (Figure 2) contain the most power with respect to periods between 1–2 solar rotations. An important feature is how the intermediate-term variations in Figure 12 begin at about 300–400 days during the rising portion of solar cycle 21, show a spectral peak near 150 days in August 1980, proceed to about 120 days during September 1981, return to about 150 days near September 1982, and continue back down to over 300 days by April 1984. The increase in frequency of these intermediate-term variations begins again during the rise of solar cycle 22. Figure 2 shows another unique feature of X_b: isolated periodicities occur that range from as low as 18 days to as high as 40 days.

4.2. 10.7 cm radio flux

In Figures 3 and 13, $F_{10.7}$ shows properties similar to the dynamic power spectra of UV indices, particularly the 27-day rotational periodicities. Tobiska and Bouwer (1989) present evidence suggesting that the dynamic power spectra of $F_{10.7}$ are most like spectra of chromospheric indices, with minor coronal properties. The differences observed between $F_{10.7}$ and X_b in this analysis are: (1) the duration of spectral peaks near 27–28 days is shorter for X_b than it is for $F_{10.7}$; (2) the wide variation in the range of frequencies near short-term periodicities is less extreme for $F_{10.7}$ than for X_b, varying within the range of about 20–36 days instead of 18–40 days; and (3) the mid-range variations seem to contain less relative power in $F_{10.7}$ than in X_b, although the intermediate-term variations are similar in frequency over time.

4.3. He I 1083 nm

Features common to the dynamic power spectra of chromospheric indices become evident upon examination of He I in Figures 4 and 14. First, more power results from the rotational periodicities as compared to intermediate-term and mid-range variations. Second, 13-day periodicities related to solar rotation and the approximately 180° separation of active regions (see details by Donnelly and Puga, 1991) become evident,

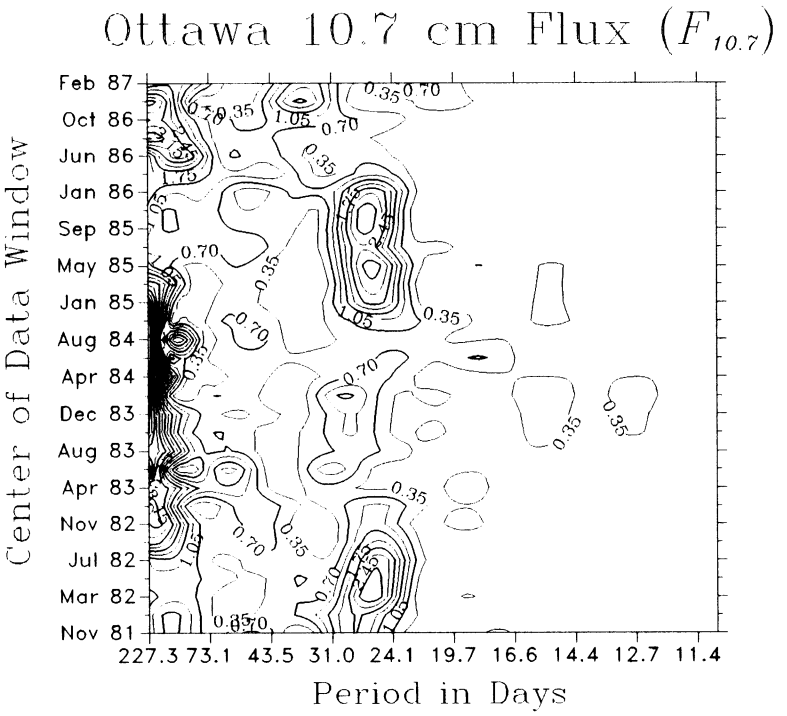

Fig. 3. Dynamic power spectra of the Ottawa 10.7 flux, emphasizing short-term periodicities related to solar rotation. Contour levels are in units of percent of total power, or a data transform window 256 days long, stepping every 64 days.

especially in February 1984. Third, periodicities vary less in frequency and are longer in duration than other solar indices. Comparing He I to $R_{Mg\,II}$ (Figures 4 and 6), the most important difference is the number of distinct spectral peaks due to solar rotation and their time of occurrence in the contour diagram. Note that He I has five distinct spectral peaks near 27–28 days compared to the seven of $R_{Mg\,II}$, of which only the May 1984, peak occurs simultaneously with $R_{Mg\,II}$. Furthermore, He I fails to indicate a 13-day spectral peak during April 1983, when a number of other solar indices confirm its presence. Another distinction of He I is that its intermediate-term variations usually are on the order of 200–600 days (Figure 14) throughout cycle 21, when in most other indices the intermediate-term variations are as low as 100 days.

4.4. SME Lα

The dynamic power spectra for Lα, shown in Figure 5, correspond closely to that of $R_{Mg\,II}$ (Figure 6), with three exceptions. First, there is a lack of fine resolution of its five rotational spectral peaks in comparison to the seven spectral peaks of $R_{Mg\,II}$, especially during 1984. Second, the relative power in Lα of the 13-day periodicity during 1983 and 1984 is not as strong as it is with most other solar UV indices. Third, most other solar indices in this study show distinct periods near 36 days early in 1987 that are absent

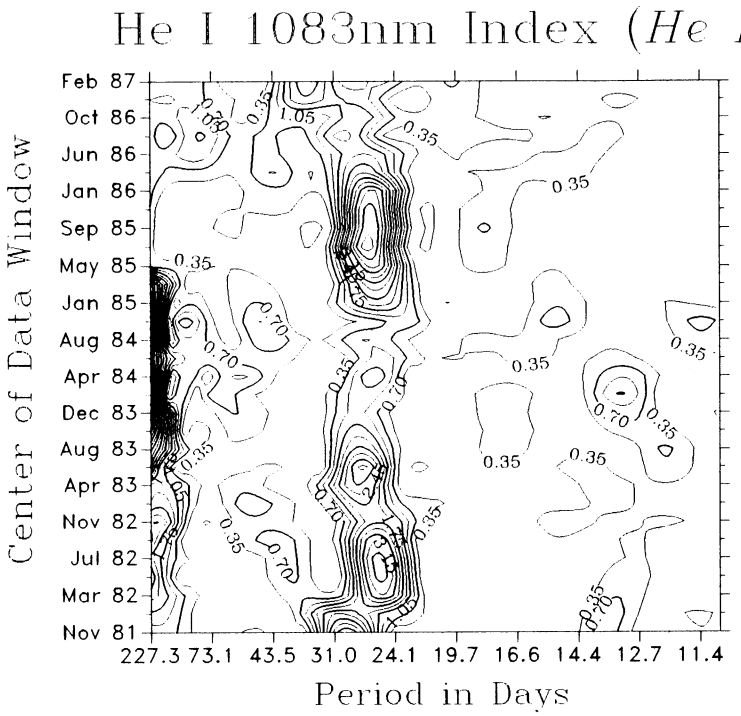

Fig. 4. Dynamic power spectra of the He I line, emphasizing short-term periodicities related to solar rotation. Contour levels are in units of percent of total power, for a data transform window 256 days long, stepping every 64 days.

from Lα. Except for these differences Lα is similar to $R_{\mathrm{Mg\,II}}$, especially regarding rotational periods.

4.5. Mg II CENTER-TO-WING RATIO

Figure 6 shows the detailed dynamic power spectra of $R_{\mathrm{Mg\,II}}$. Each spectral peak in the band of rotational periodicities suggests a distinct peak in active-region evolution. One particularly long-lived periodicity is the 27-day period that persisted for all of 1985 and part of 1986. In addition to the seven distinct spectral peaks near 27–28 days, there are two distinct peaks near 13–14 days during 1983–1984. The modulation of the rotational period between 26 to 28 days during 1982–1983 is evident. Similarly, the change in the approximately 14-day period in April 1983, to nearly 13 days in February 1984, is also apparent. Of all the indices, $R_{\mathrm{Mg\,II}}$ seems to have the best measurement signal-to-noise ratio, resulting in very detailed dynamic power spectra.

4.6. Ca-K PLAGE INDEX

Ca-K in Figures 7 and 15 begins to show a greater variation in its dynamic power spectra, which seems characteristic of indices more related to strong magnetic fields than to chromospheric emission. Several mid-range variations between about

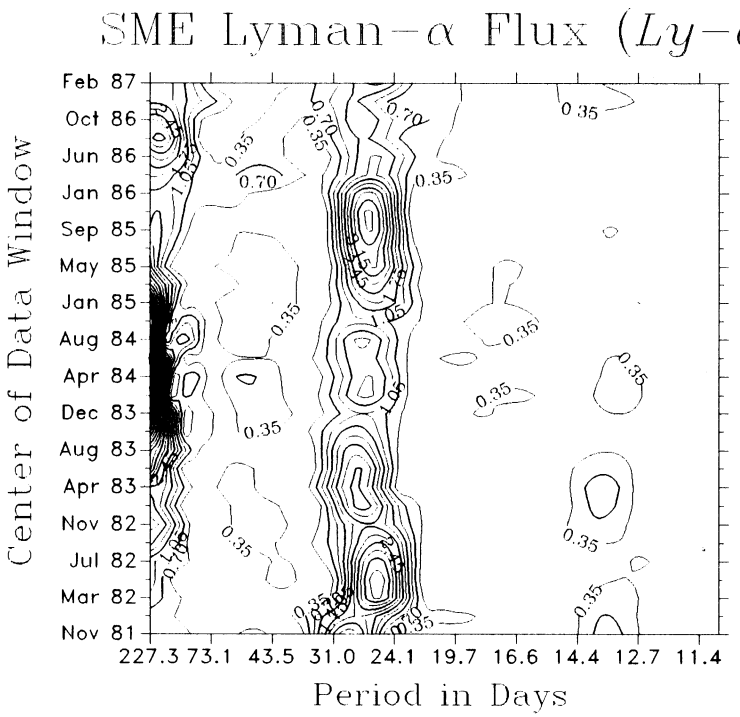

Fig. 5. Dynamic power spectra of the SME Lα flux, emphasizing short-term periodicities to solar rotation. Contour levels are in units of percent of total power, for a data transform window 256 days long, stepping every 64 days.

39–71 days emerge (Figure 7). Late in 1986, a strong 38-day spectral peak (noticeable at the top border in Figure 7) appears in Ca-K. This peak coexists with a weak, 22-day period in a fashion similar to that of $F_{10.7}$, and less obviously S_{act} and S. During 1981–1985, the Ca-K contours appear most similar to UV indices (e.g., Lα and $R_{Mg\,II}$). During 1986–1987, the Ca-K contours begin to resemble indices related to strong magnetic fields (e.g., PSI and S_{act}). Except near solar maximum in 1980–1981, the intermediate-term variations (Figure 15) of Ca-K are similar to the intermediate-term variations of $F_{10.7}$ (Figure 13).

4.7. Total Solar Irradiance

Describing the chaotic appearance of S in Figure 8 is difficult. If many of its spectral peaks did not coincide in a subtle fashion with a number of spectral peaks in S_{act}, S_{pas}, and PSI, and if a separate analysis of recent NIMBUS-7 ERB data (not shown here) did not confirm the majority of SMM/ACRIM spectral peaks, one would be inclined to consider its dynamic power spectra as representative of a random process.

Between February and December 1980 and after May 1984, the SMM data are more precise than during the 1981–1983 portion of the time series. This is because the solar pointing system of the satellite failed from 1981–1983 (see details in Paper I, or in

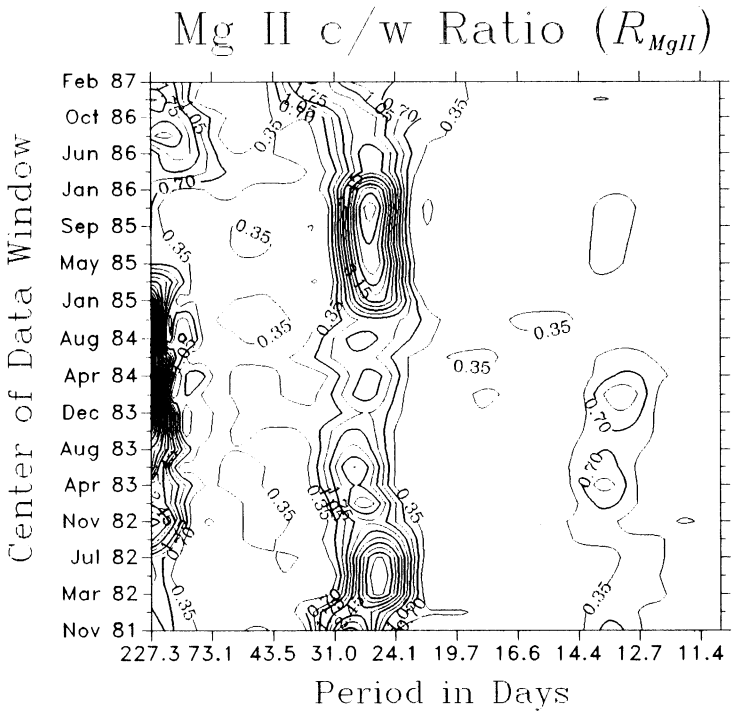

Fig. 6. Dynamic power spectra of the Mg II center-to-wing ratio, emphasizing short-term periodicities related to solar rotation. Contour levels are in units of percent of total power, for a data transform window 256 days long, stepping every 64 days.

Willson and Hudson, 1991). Nevertheless, the principal observations of the dynamic power spectra of S shown in Figure 8 are: (1) the complicated periodicities at sidebands of rotational periods during the declining portions of cycle 21, (2) the rotational periods near 22 days during the early 1985 portion of solar minimum, and (3) the sudden change of the apparent rotational period to nearly 26 days during the late-1986 portion of solar minimum. Figure 8 also shows a major episode of the 13-day period in 1983.

4.8. Photometric Sunspot Index

The most dramatic features of PSI (Figure 9) are: (1) the relatively powerful spectral peaks during solar minimum at 26 days and at about 40 days, (2) the multiple 13–15-day periods in 1983–1985, and (3) the similar intermediate-term variations to X_b and S_{act}. Carefully comparing the PSI contour figures to the S_{act} and S_{pas} figures, it is possible to see how the PSI structure in the contour figures corresponds in time and frequency (but not amplitude due to limb-darkening effects) to the combined effects of S_{act} and S_{pas}. Note how the relative effects of S_{pas} are most pronounced in PSI during solar minimum, when mainly old sunspots are on the Sun.

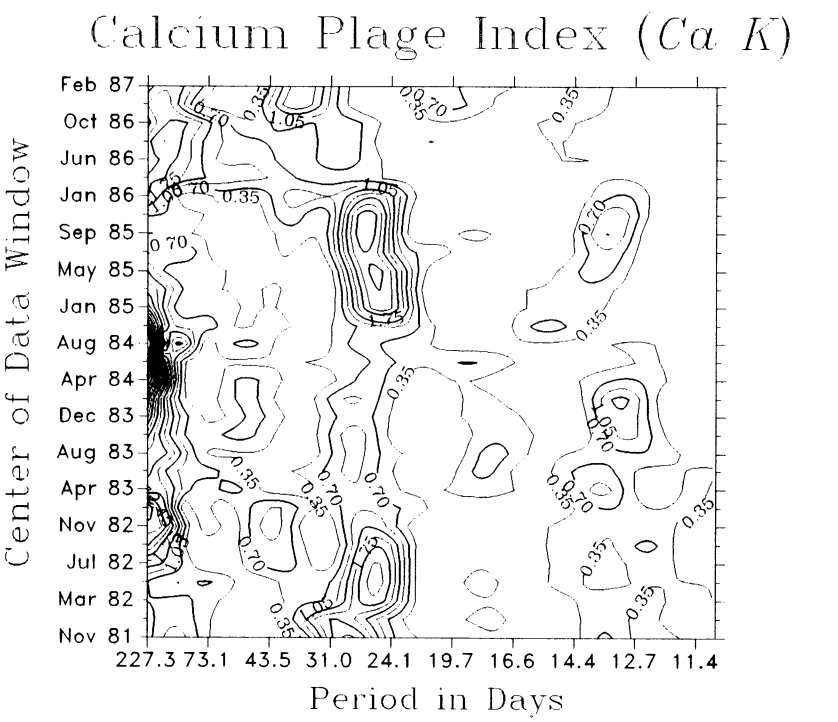

Fig. 7. Dynamic power spectra of the calcium plage index, emphasizing short-term periodicities related to solar rotation. Contour levels are in units of percent of total power, for a data transform window 256 days long, stepping every 64 days.

4.9. Projected Area of Active Sunspots

S_{act} in Figure 10 shows many features similar to X_b. There is a greater modulation of the rotational periods in S_{act} than in chromospheric indices. There is a splitting near 13–14 days in 1983, as in X_b and $F_{10.7}$. Note the relative weakness of rotational periods during the descending portion of cycle 21 (i.e., 1983–1984), when intermediate-term variations dominate the power spectra. During 1981–1982 the rotational period is at about 27 days, abruptly ending early in 1983. During 1984, nearly all the power in S_{act} is found in intermediate-term variations. For about four months during the 1985–1986 solar minimum, S_{act} shows a strong 26–27-day period.

4.10. Projected Area of Passive Sunspots

Comparing S_{pas} in Figure 11 to S_{act} in Figure 10 illustrates the dramatic differences between the two sunspot indices. During the descending portion of the solar cycle up to 1985, the power spectra S_{act} and S_{pas} are mutually exclusive; where a periodicity is strong in one index, it is absent in the other. From 1982 to 1985, S_{pas} has virtually no power at rotational periods, but instead shows nearly all its power at periods between 32 to about 53 days. Then, in March 1985 and later in January 1986 S_{pas} shows a strong rotational period at 26 days. Finally, in mid-1986 the rotational period of S_{pas} splits into

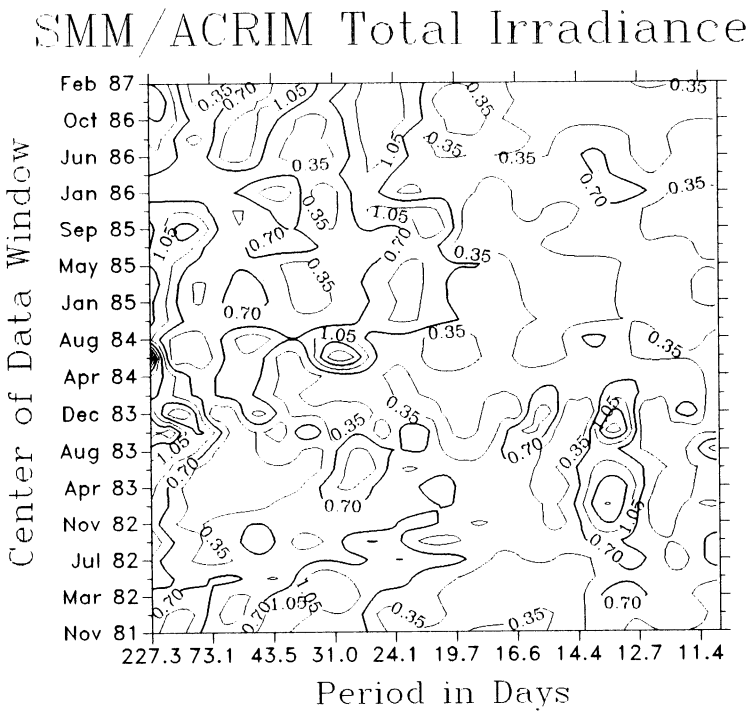

Fig. 8. Dynamic power spectra of the SMM/ACRIM total solar irradiance, emphasizing short-term periodicities related to solar rotation. Contour levels are in units of percent of total power, for a data transform window 256 days long, stepping every 64 days.

two distinct spectral peaks at 22 and 32 days. During the ascending part of cycle 22 in 1987, S_{pas} continues to show a short-term period near 28 days, while S_{act} has a strong spectral peak at 36 days.

5. Discussion of Common Spectral Peaks

A number of spectral peaks occur in common among the indices, from short-term periodicities to intermediate-term variations. I begin by noting in Figures 2–11 that the 12–14-day period is most obvious in measurements related to chromospheric emission (i.e., He I, Lα, $R_{Mg\,II}$, and Ca-K), with the clearest signature in Ca-K. It is also observed at lower relative power in X_b, S_{act}, S_{pas}, and PSI. The 12–14-day period is strongly present in S on at least two occasions coincident with similar periods in UV measurements. From 1979 to 1986, collectively there are 3 major episodes of 12–14-day periodicity: (1) February–March 1979, (2) February–May 1984, and (3) April–May 1988. Note that during 1984 the power in the 12–14-day period is greatest when the 26–28-day period is comparatively weak. It is important to recall that the 12–14-day period is not due to a phase-related harmonic from the power spectra of a single peak per rotation in the time series. Instead, the 12–14-day period is often due to the

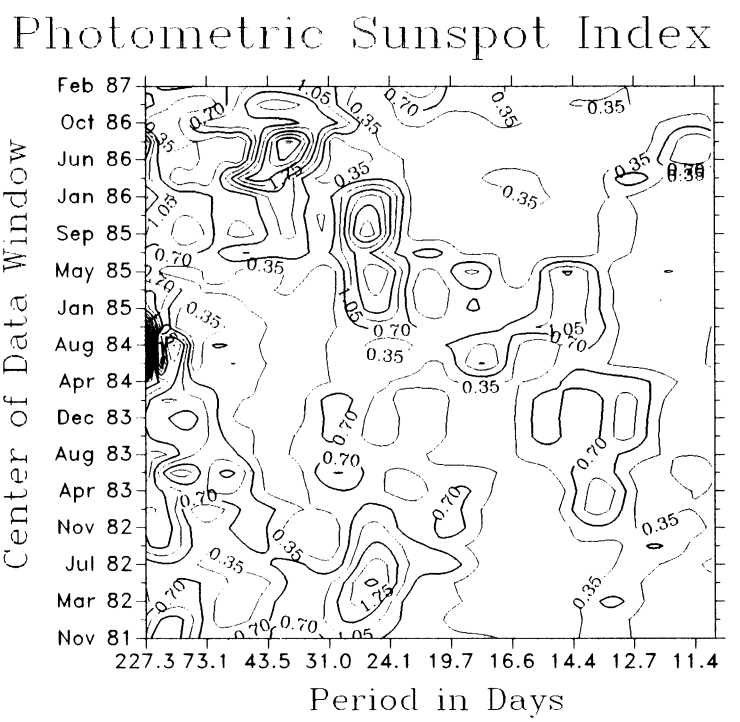

Fig. 9. Dynamic power spectra of the photometric sunspot index, emphasizing short-term periodicities related to solar rotation. Contour levels are in units of percent of total power, or a data transform window 256 days long, stepping every 64 days.

observation of two peaks per rotation, resulting from two active regions separated by roughly 180° in longitude (Donnelly, 1982, 1988; Donnelly and Puga, 1991). Donnelly has also shown (Donnelly *et al.*, 1985) that the 12–14-day period is generally present in chromospheric indices but absent in $F_{10.7}$, which is confirmed here.

Examining Figures 2–11, rotational variations near 26 days dominate most measurements in two major episodes: (1) March 1982–October 1982 and (2) January 1985–February 1986. The rotational period seen in chromospheric indices is the most dramatic spectral peak, clearly showing a single dominant periodicity of nearly constant frequency and amplitude. $R_{\mathrm{Mg\,II}}$ shows the most fine structure at rotational periods in the contour figures, suggesting that it best shows the emergence and subsequent evolution of active regions in the chromosphere. Other instances of rotational variations at lower relative power can be found in concurrent data series, especially between He I, Lα, and $R_{\mathrm{Mg\,II}}$; often the relative power of a period is strong in one measurement but not in the other. For example, in mid-1983 there is a distinct rotational spectral peak at 28 days in $F_{10.7}$, He I, Lα, and $R_{\mathrm{Mg\,II}}$ that is weaker or absent in the other indices. However, there are several interesting points regarding rotational periodicities.

Generally, the contour figures demonstrate that periodicities range from a low of 20 days to a high of 36 days. The most evident 36-day period in nearly all solar indices

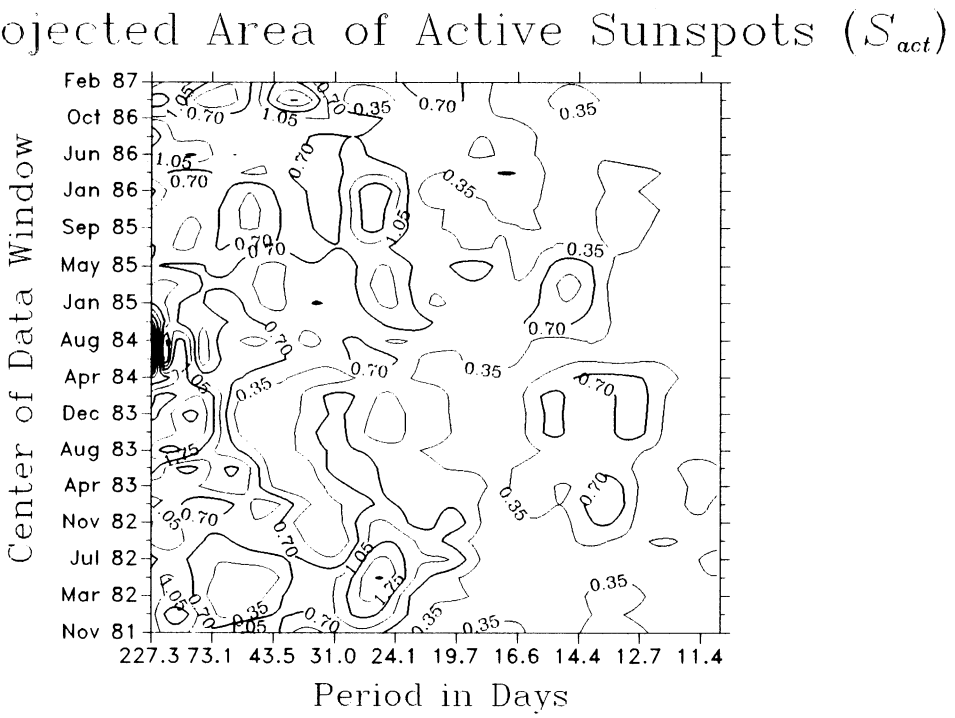

Fig. 10. Dynamic power spectra of active sunspot areas, emphasizing short-term periodicities related to solar rotation. Contour levels are in units of percent of total power, for a data transform window 256 days long, stepping every 64 days.

occurs late in 1981 and early in 1987. I cannot offer an obvious explanation for the wide variation in what may appear to be related to rotational rates, but I observe that the greatest variation occurs in indices related to strong magnetic fields and coronal emission (e.g., X_b, PSI, S_{act}, and S_{pas}). In the dynamic spectral analysis, the large variations in rotational periodicities will influence the spectral amplitudes and change the frequencies due to these evolutionary effects. However, one explanation for a 36-day period may be that the distribution of numerous active regions over a wide range of longitudes, coupled with their peak emission at different times in their evolution, coincidentally forms a 36-day period. An additional explanation might be the periodicities resulting from the *r*-modes and *g*-modes of global oscillations discussed by Wolf (1983, 1984, 1987). Not only does Wolf predict several periods in total solar irradiance at less than 21 days and near 36 days due to *g*-modes, but he also suggests periodicities throughout the range of 37 to about 670 days due to the combination of *g*-modes, *r*-modes, and solar rotation.

Nonetheless, an important feature in the dynamic power spectra is that nearly all the indices with periodicities around 30–34 days shift to about 26–28 days during 1982 (see He I, Lα, $R_{\text{Mg II}}$, and Ca-K). After examining spatial solar data and finding that major active regions are at less than about 25° latitude, I conclude that this increase in the

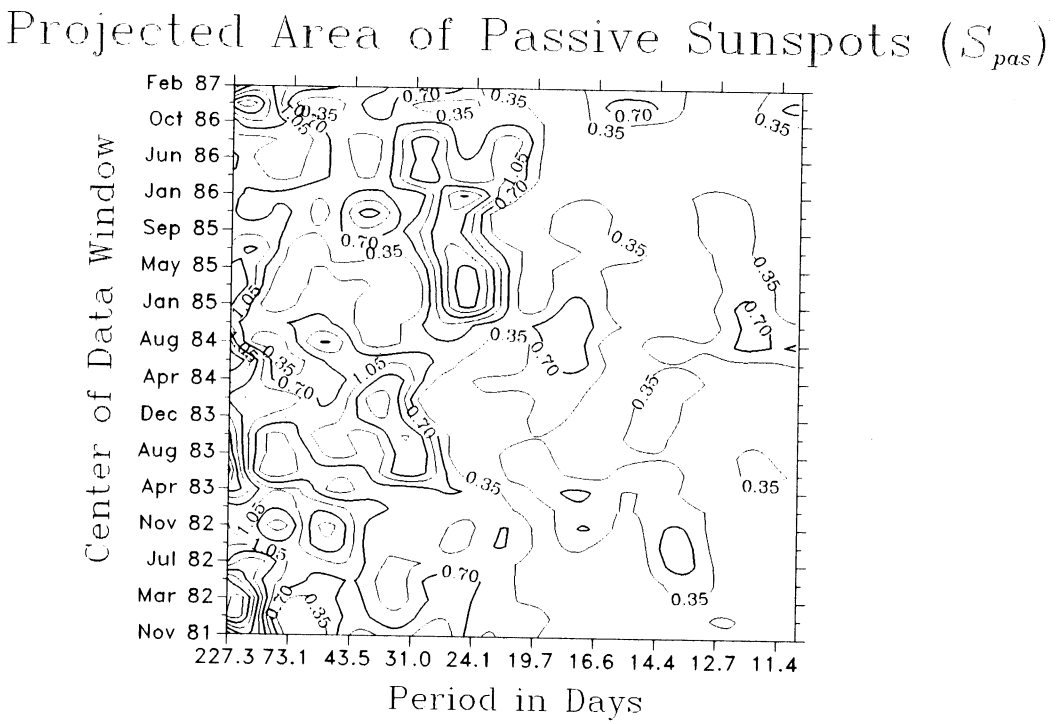

Fig. 11. Dynamic power spectra of passive sunspots, emphasizing short-term periodicities related to solar rotation. Contour levels are in units of percent of total power, for a data transform window 256 days long, stepping every 64 days.

apparent rotational period is due to the combination of active-region evolution and solar rotation (i.e., not due to differential rotation). As older active regions rotate across the visible solar disk, new active regions form at widely spaced longitudes from the older regions; this creates a periodicity in the power spectra up to about 6 days different from a 27–28-day rotational period. Thus the formation of new active regions at widely separated longitudes can result in apparent rotational periods from about 20 to 36 days.

Note that spectral peaks at rotational periods persist at nearly constant frequency and amplitude for up to about 12 solar rotations in a few indices, particularly near the solar rotation period. For example, the duration of a particular spectral peak in Lα and $R_{\mathrm{Mg\,II}}$ may persist in the contour plots for up to 8–12 solar rotations; in most other measurements the periodicities seldom persist for more than 4–8 rotations. In other words, the chromospheric time series suggest stationarity on time scales up to about 8–12 solar rotations, while most other time series (particularly those possibly related to strong magnetic fields), suggest stationarity on intermediate-term time scales (i.e., 3–8 solar rotations).

An intriguing result becomes evident when the apparent rotation rates of indices related to chromospheric emission are compared; there are only three instances during solar cycle 21 when the apparent solar rotation rates for all indices are in very close

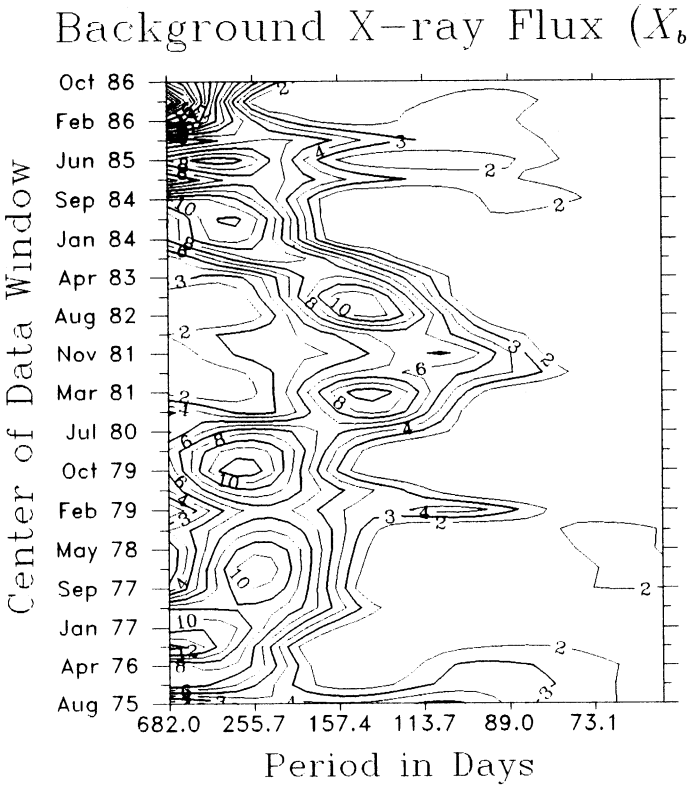

Fig. 12. Dynamic power spectra of background X-ray index, emphasizing intermediate-term variations related to active region formation and evolution. Contour levels are in units of percent of total power, for a data transform window 512 days long, stepping every 128 days.

agreement (early 1980, 1982/1983, 1985), as shown in Figure 16. $F_{10.7}$ is the least chromospheric of the indices used, but it is more consistent with chromospheric variations than with coronal variations. X_b, S, S_{act}, S_{pas}, and PSI all have a wide variation in periodicities near 27–28 days, without an obvious pattern. Carefully examining Figures 3 to 7, it can be seen that each spectral peak for $F_{10.7}$ and the chromospheric indices differ not so much in the frequency of its period but more in the time it occurs. For example, note that during the descending portion of cycle 21 the spectral peak of $F_{10.7}$ occurs just slightly before the R_{MgII} spectral peak. This finding is consistent with the results of Donnelly (1992), who found in several instances that $F_{10.7}$ peaks early in active region evolution on the first rotational peak and decreases on subsequent rotations, while UV tends to peak on the second rotational maximum and decreases more slowly than $F_{10.7}$. Part of the reason for the more gradual decrease in UV flux is that as active regions decay, the remnants of plages still influence UV irradiance (Pap, Marquette, and Donnelly, 1991).

The 51–52-day period is an enigma: is it due to an alternating 25–26-day period, or does it represent a completely different process? The 51–52-day period has been

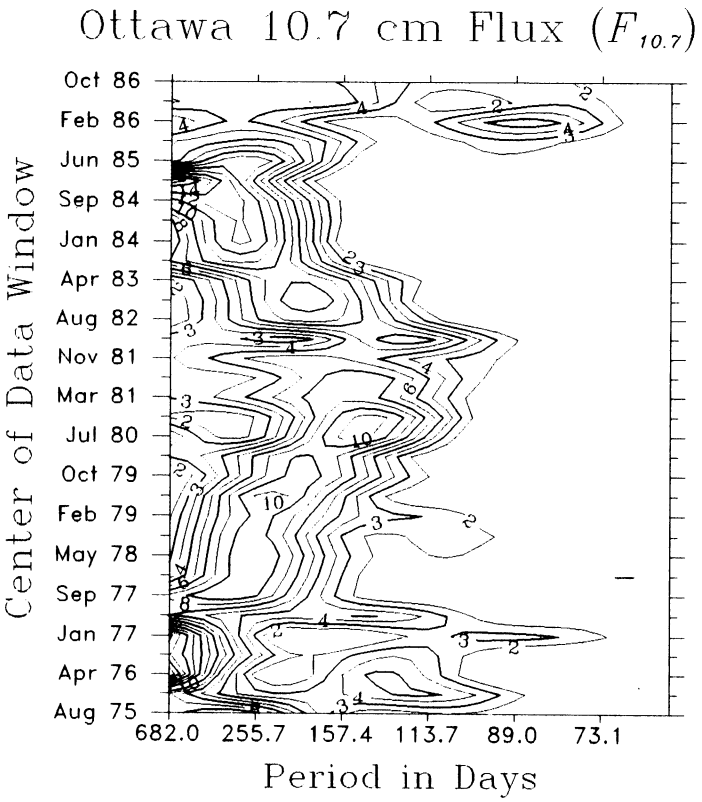

Fig. 13. Dynamic power spectra of the Ottawa 10.7 cm flux, emphasizing intermediate-term variations related to active region formation and evolution. Contour levels are in units of percent of total power, for a data transform window 512 days long, stepping every 128 days.

reported before (Fröhlich and Pap, 1989; Gabriel, Evans, and Feynman, 1990; Lean and Brueckner, 1989; Bai, 1987a, b; Kile and Cliver, 1992). The relative persistence of the 51-day period in measurements related to emerging magnetic fields is discussed by Bouwer, Donnelly, and Pap (1990) using an earlier, less developed, and more phase-dependent version of the dynamic power spectra. In this study, I find that from 1980 to 1986 the 51–52-day period is present at least three times in all data sets analyzed. However, the 51–52-day period is not always present in all data sets simultaneously, and it usually appears at very low power. It appears most strongly in those measurements closely related to emerging magnetic flux (e.g., S_{act} in Figure 10). The 51–52-day period also appears at different times in S, S_{pas}, and PSI.

Another interesting feature of the 51–52-period not explicitly shown in this paper is its phase coherency. In several measurements, when the restrictions on analyzing quasi-stationary time series are relaxed and an FFT is performed on the entire time series, the 51–52-day period becomes one of the strongest periods. The increase in the relative power of the 51–52-day period when analyzing long solar time series indicates

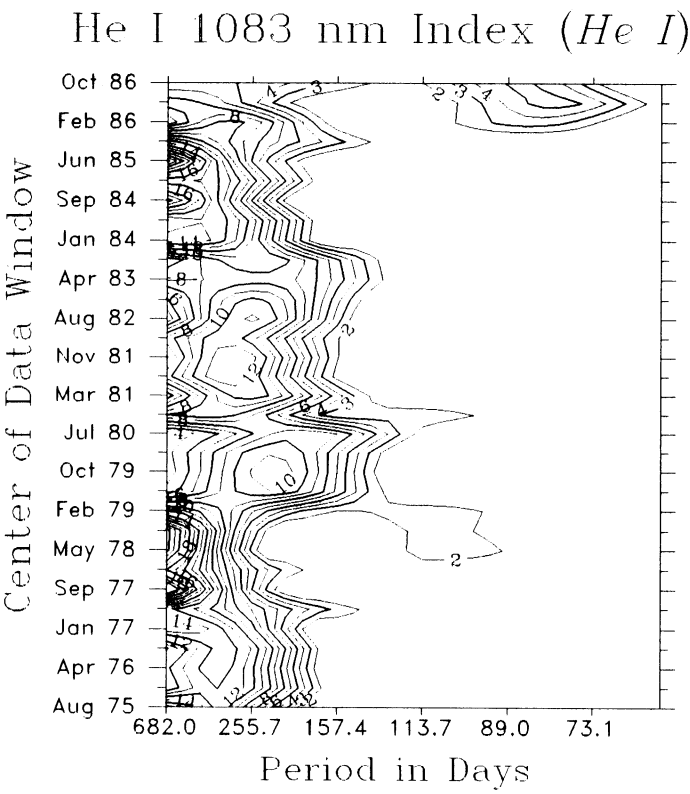

Fig. 14. Dynamic power spectra of the He I line, emphasizing intermediate-term variations related to active region formation and evolution. Contour levels are in units of percent of total power, for a data transform window 512 days long, stepping every 128 days.

that the 51–52-day period is the most phase-coherent of the periodicities over long time intervals. After examining the results, Wolf (1991, private communication) could not relate the 51–52-day period to any predicted *g*-mode oscillations, which might have explained the phase coherence of the 51-day period.

Examining Figures 12–15 I conclude that, with a single possible exception, there are no convincing observations of periodicities on intermediate-term time scales. The exception may be an approximately 154-day period ($\pm$ 13 days) that is temporarily present in X_b, $F_{10.7}$, $R_{\mathrm{Mg\,II}}$, Ca–K, S_{act}, and PSI during the 1980 and 1982 time frames. In these cases, the period has a higher percentage power in indices related to strong, emerging magnetic fields (e.g., X_b, Figure 2). However, other spectral peaks on intermediate-term time scales are observed. For example, there is a single case of a 81–95-day spectral peak during 1986 that is present to some degree in all the measurements except Lα and *S*, and a single case of an approximately 340-day period during 1984 that is present in all the measurements to some degree. Kile and Cliver (1992) summarize a number of prior studies of the 154-day period, and conclude that the evidence for the

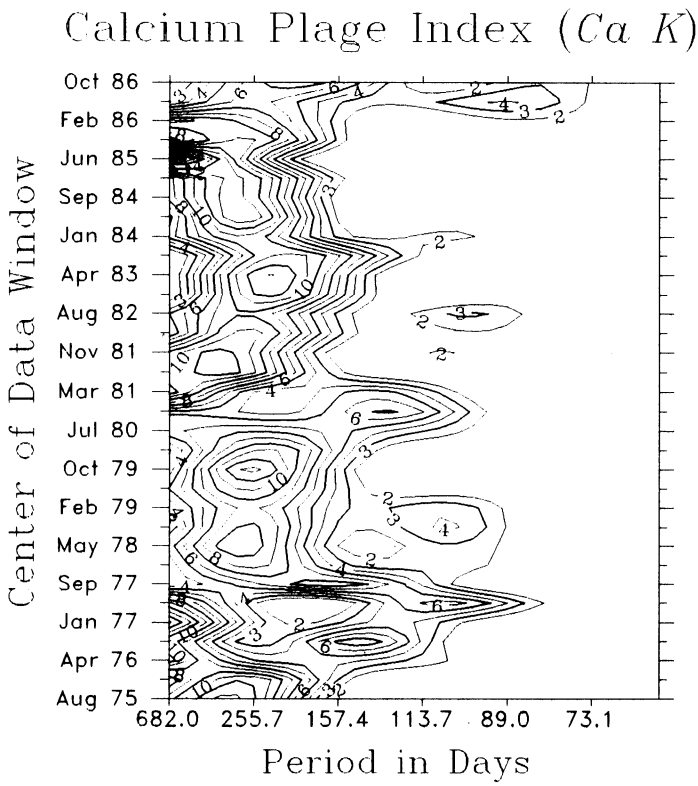

Fig. 15. Dynamic power spectra of the calcium plage index, emphasizing intermediate-term variations related to active region formation and evolution. Contour levels are in units of percent of total power, for a data transform window 512 days long, stepping every 128 days.

154-day period in non-flare-related data sets is contradictory; however, these authors discuss convincing evidence for the 154-day period during 1978–1983 in flare-related data. A 153–157-day period has also been reported by Rieger (1984), Kiplinger, Dennis, and Orwig (1984), Bogart and Bai (1985), Ichimoto *et al.* (1985), Lean and Brueckner (1989), and Bai and Cliver (1990). In this study, there is insufficient correlation of spectral peaks between the indices analyzed, their observed periods, and the dates of occurrence of spectral peaks to detect an obvious pattern. The appearance of a 154-day period could be the result of a coincidental occurrence of one or more non-periodic waveforms, and not the result of a true solar periodicity.

6. Conclusions

The time-varying nature of the dynamic power spectra of 10 different indices of solar time series measurements suggests that quasi-stationary processes dominate solar activity. In all cases, the presence of a particular spectral power peak is temporary, and the power spectra evolve over the solar cycle. Measurements of chromospheric data are

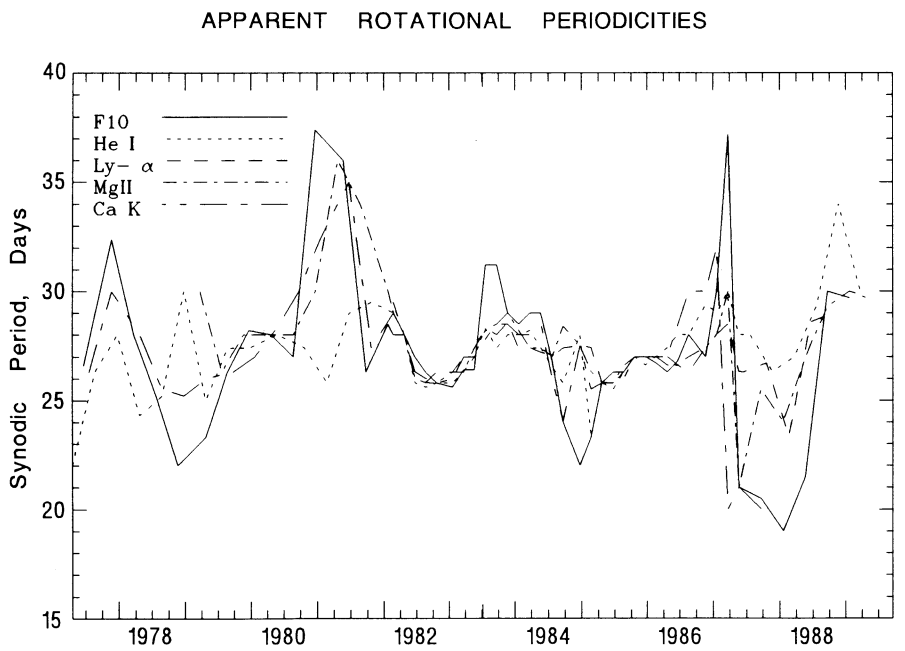

Fig. 16. The apparent rotation rates derived from the dynamic power spectra (Figures 2–11) of chromospheric indices, illustrating the effect of two or more evolving active regions modulating the periodicity due to solar rotation.

the most stationary, while the measurements of data associated with strong solar magnetic fields are the least stationary. It is more accurate to use the term quasi-stationary for both cases of solar time series because often there are time intervals that might be closely approximated with stationary statistics.

Spectral peaks that come and go on the contour plots reflect the formation of active regions at new longitudes and the subsequent rotational modulation of signal produced by these active regions evolving over time. Statistically, when a solar time series less than about 1–2 years is analyzed with a power spectrum, most individual periodicities appear significant. However, when a solar time series longer than about 2 years is analyzed, loss of phase coherence, changing variance, and other non-stationary effects obscure the spectrum.

Another important general observation is how different the dynamic power spectra appear between the solar source regimes (i.e., coronal, chromospheric, and photospheric). From short-term to intermediate-term time scales there are large differences between the dynamic power spectra of the data from various solar source regimes. These differences are large enough to support the hypothesis that a measurement from one solar source regime cannot easily be used as a proxy measurement for another regime because each index to solar variability encompasses a unique set of physical mechanisms.

The periodicities ranging between 20–36 days are dominated by what appears to be

solar rotation near 27–28 days for most of the time, especially in the chromospheric indices. However, one does not expect a range of periodicities solely due to solar rotation greater than 24–30 days. The combination of two or more active regions widely separated in longitude and at different stages of evolution modulate the apparent solar rotation visible in the time series. Chromospheric indices (i.e., $F_{10.7}$, HeI, Lα, R_{MgII}, and Ca-K) demonstrate greater stationarity than indices related to strong magnetic fields (i.e., X_{b}, S_{act}, S_{pas}, S, and PSI), as demonstrated by their periodicities persisting for up to 8–12 solar rotations at relatively constant amplitude and frequency. In contrast, coronal, total irradiance, and sunspot indices usually do not persist for more than three solar rotations, and are highly variable in frequency and amplitude. Other important considerations are the optical thickness of the solar atmosphere to active-region emissions, the height in the solar atmosphere of the emission source, and the central meridian dependence (CMD) of a particular solar index from a terrestrial viewpoint (Donnelly, 1987). For example, Donnelly has shown that the X-ray CMD curve appears as a square wave, while many chromospheric and photospheric indices appear as a cosine wave. It will be necessary to carefully examine related spatial information to gain additional insight into the physics of this wide range of short-term periodicities.

Any conclusions regarding the 51–52-day period are not possible at this point other than to emphasize its frequent recurrence in a variety of solar indices at low amplitude, its suggested phase stability, and its strong association with indices related to emerging magnetic flux. It is unlikely that this represents a harmonic or sub-harmonic of other periodicities because there are several instances when it is present or particularly strong, and other harmonic periodicities are either weak or absent.

The results suggest the temporary existence of an approximately 154-day period during portions of the solar cycle, and indicate that it appears most strongly in those indices related to strong emerging magnetic fields. However, many other spectral peaks related to intermediate-term variations range from about 81 to 400 days, which may represent non-periodic or transient waveforms because of their lack of persistence over long time scales and their isolated occurrence. A dynamic power spectra of flare-related data over more than a solar cycle may make a stronger case for the 154-day period.

I suggest that the quasi-stationary nature of the data, coupled with undesirable spectral effects from commonly-used analysis algorithms, might mislead one into over-estimating or underestimating the significance of a spectral peak. Another effect of quasi-stationarity can be very apparent in simple linear regressions of solar indices over two or more intermediate-term episodes of activity: often the residuals resulting from the regression demonstrate a high degree of autocorrelation. This in turn suggests that, despite relatively high correlation coefficients, simple linear models between solar indices may not be accurate. The effects of quasi-stationarity on solar time series analysis can be reduced by analyzing segments of time less than 2 years long. In the case of spectral peaks at periodicities longer than rotational periodicities, often a significant peak in the power spectra does not necessarily imply a periodicity; other non-cyclic waveforms may also generate spectra peaks with large power.

Acknowledgements

A special thanks to Dr J. Pap for use of the active and passive sunspot data, and her many useful comments and contributions; this paper would not have been possible without her assistance. Drs R. C. Willson, H. L. Kyle, D. Heath, and G. Rottman provided the SMM/ACRIM, NIMBUS-7 SBUV, and SME Lyman alpha data. Dr H. S. Hudson provided the PSI data, and J. Harvey the He 1083 data, which are produced cooperatively by NSO/NOAO, NASA/GSFC, and NOAA/SEL. Discussions with O. R. White, A. Kiplinger, D. Lewis, and N. Crow were crucial to the analysis. I am very grateful to Dr R. F. Donnelly for his support and direction, and the use of the NOAA SBUV data. This research was supported by a grant of the NOAA Space Environment Laboratory while the author was employed with the Cooperative Institute for Research in the Environmental Sciences (CIRES), University of Colorado.

References

Bai, T.: 1987a, *Astrophys. J.* **318**, L85.
Bai, T.: 1987b, *Astrophys. J.* **314**, 795.
Bai, T. and Cliver, E. W.: 1990, *Astrophys. J.* **363**, L299.
Barth, C. A., Tobiska, W. K., and Rottman, G. J.: 1990, *Geophys. Res. Letters* **17**, 571.
Bath, M.: 1974, *Spectral Analysis in Geophysics*, Elsevier Sci., Amsterdam, p. 125.
Bloomfield, P.: 1976, *Fourier Analysis of Time Series: An Introduction*, John Wiley and Sons, New York, p. 84.
Bogart, R. S. and Bai, T.: 1985, *Astrophys. J.* **299**, L51.
Bouwer, S. D.: 1983, *J. Geophys. Res.* **88**, 7823.
Bouwer, S. D., Donnelly, R. F., and Pap, J.: 1990, in K. H. Schatten and A. Arking (eds.), *Climate Impact of Solar Variability*, NASA Conf. Publ. 3086, p. 125.
Bouwer, S. D., Donnelly, R. F., Falcon, J., Quintana, A., and Caldwell, G.: 1982, *NOAA Tech. Memo ERL SEL-62*, NOAA ERL, Boulder, Colorado.
Daubechies, I.: 1990, *IEEE Trans. on Info, Theory* **36**, 961.
Dodson, H. W. and Hedeman, E. R.: 1970, *Proceedings of Observations and Prediction of Solar Activity Conference*, Am. Inst. of Aeronaut. and Astronaut., Huntsville, Alabama, p. 1368.
Donnelly, R. F.: 1987, *Solar Phys.* **109**, 37.
Donnelly, R. F.: 1988, *Ann. Geophys.* **6**, 417.
Donnelly, R. F.: 1989, in J. Laštovička (ed.), *MAP Handbook* **29**, 1.
Donnelly, R. F.: 1992, in K. Cole *et al.* (eds.), *J. Geomag. Geoelect.* (in press).
Donnelly, R. F. and Puga, L. C.: 1990, *Solar Phys.* **130**, 369.
Donnelly, R. F., Harvey, J. W., Heath, D. F., and Repoff, T. P.: 1985, *J. Geophys. Res.* **90**, 6267.
Fröhlich, C. and Pap, J.: 1989, *Astron. Astrophys.* **220**, 272.
Gabriel, S., Evans, R., and Feynman, J.: 1990, *Solar Phys.* **128**, 415.
Harvey, J. W.: 1980 in S. Sofia (ed.), *Variations of the Solar Constant*, NASA Conf. Publ. 2191, p. 197.
Harvey, J. W.: 1984, in B. J. LaBonte *et al.*, (eds.), *Solar Irradiance Variations on Active Region Time Scales*, NASA Conf. Publ. 2310, p. 197.
Heath, D. F. and Schlesinger. B. M.: 1986, *J. Geophys. Res.* **91**, 8672.
Heath, D. F., Repoff, T. P., and Donnelly, R. F.: 1984, *NOAA Tech. Memo. ERL ARL-129*, Air Resources Lab., NOAA ERL, Boulder, Colorado.
Hudson, H. S.: 1988, *Ann. Rev. Astron. Astrophys.* **26**, 473.
Ichimoto, K., Kubota, F., Suzuki, M., Tohmura, L., and Kurokawa, H.: 1985, *Nature* **315**, 422.
Karlický, M.: 1977, *Bull. Astron. Inst. Czech.* **28**, 200.
Kile, J. N. and Cliver, E. W.: 1992, *Astrophys. J.* **370**, 442.
Kiplinger, A. L., Dennis, B. R., and Orwig, L. E.: 1984, *Bull. Ann. Astron. Soc.* **16**, 891.
Kotz, S. and Johnson, N. L. (eds.): 1983, *Encyclopedia of Statistical Sciences*, Vol. **3**, John Wiley and Sons, New York, p. 118.

Koopmans, L. H.: 1974, *The Spectral Analysis of Time Series*, Academic Press, New York, p. 38.
Lean, J. L. and Brueckner, G. E.: 1989, *Astrophys. J.* **337**, 568.
Lean, J. L. and Repoff, T. P.: 1987, *J. Geophys. Res.* **92**, 5555.
Lean, J., White, O. R., Livingston, W. C., Heath, D. F., Donnelly, R. F., and Skumanich, A.: 1982, *J. Geophys. Res.* **87**, 10,307.
Pap, J.: 1986, *Astrophys. Space Sci.* **127**, 55.
Pap, J., Tobiska, W. K., and Bouwer, S. D.: 1990, *Solar Phys.* **129**, 65.
Pap, J. M., Marquette, W. H., and Donnelly, R. F.: 1991, *Adv. Space Res.* **91**, 11, 271.
Papoulis, A.: 1977, *Signal Analysis*, McGraw-Hill, New York, p. 300.
Ribes, E., Merlin, P., Ribes, J. C., and Barthalot, R.: 1989, *Ann. Geophys.* **7**, 321.
Rieger, E., Shane, G. H., Forrest, D. K., Kanback, G., Reppin, C., and Chupp, E. L.: 1984, *Nature* **312**, 623.
Tobiska, W. K. and Bouwer, S. D.: 1989, *J. Geophys. Res.* **16**, 779.
Wagner, W. J.: 1988, *Adv. Space Res.* **8**(7), 67.
Welsh, P. D.: 1967, *IEEE Transactions on Audio and Electroacoustics* **AU-15**, 70.
Willson, R. C. and Hudson, H. S.: 1988, *Nature* **332**, 810.
Willson, R. C. and Hudson, H. S.: 1991, *Nature* **351**, 92.
Wolf, C.: 1983, *Astrophys. J.* **264**, 667.
Wolf, C.: 1984, *Solar Phys.* **93**, 1.
Wolf, C.: 1987, *Science* **235**, 1631.